







Original Article



Right Ventricular Strain Is Associated With Increased Length of Stay After Tetralogy of Fallot Repair

Ranjini Srinivasan , MD¹, Jennifer A. Faerber, PhD², Grace DeCost, MS³, Xuemei Zhang , MS², Michael DiLorenzo , MD, MSCE⁴, Elizabeth Goldmuntz , MD⁵, Mark Fogel , MD⁵, and Laura Mercer-Rosa , MD, MSCE⁵

OPEN ACCESS

Received: Apr 21, 2021

Revised: Jul 13, 2021

Accepted: Jul 20, 2021

Published online: Aug 4, 2021

Address for Correspondence:

Ranjini Srinivasan, MD


Division of Pediatric Cardiology, Hassenfeld Children's Hospital, New York University Grossman School of Medicine, 301 E 34th Street, New York, NY 10016, USA.
Email: ranjini.srinivasan@nyulangone.org


Copyright © 2022 Korean Society of Echocardiography


This is an Open Access article distributed under the terms of the Creative Commons Attribution Non-Commercial License (<https://creativecommons.org/licenses/by-nc/4.0/>) which permits unrestricted non-commercial use, distribution, and reproduction in any medium, provided the original work is properly cited.


ORCID iDs


Ranjini Srinivasan 
<https://orcid.org/0000-0001-9567-3600>

Xuemei Zhang 
<https://orcid.org/0000-0003-0705-4231>

Michael DiLorenzo 
<https://orcid.org/0000-0002-2230-684X>

Elizabeth Goldmuntz 
<https://orcid.org/0000-0003-2936-4396>

Mark Fogel 
<https://orcid.org/0000-0001-7490-3702>

Laura Mercer-Rosa 
<https://orcid.org/0000-0003-2170-5942>

Conflict of Interest

The authors have no financial conflicts of interest.

¹Division of Pediatric Cardiology, Hassenfeld Children's Hospital, New York University Grossman School of Medicine, New York, NY, USA

²Department of Biomedical and Health Informatics, Data Science and Biostatistics Unit, Children's Hospital of Philadelphia, Philadelphia, PA, USA

³School of Public Health, Brown University, Providence, RI, USA

⁴Division of Cardiology, Morgan Stanley Children's Hospital of New York, Columbia University, New York, NY, USA

⁵Division of Cardiology, Children's Hospital of Philadelphia, University of Pennsylvania Perelman School of Medicine, Philadelphia, PA, USA

ABSTRACT

BACKGROUND: Little is known regarding right ventricular (RV) remodeling immediately after Tetralogy of Fallot (TOF) repair. We sought to describe myocardial deformation by cardiac magnetic resonance imaging (CMR) after TOF repair and investigate associations between these parameters and early post-operative outcomes.

METHODS: Fifteen infants underwent CMR without sedation as part of a prospective pilot study after undergoing complete TOF repair, prior to hospital discharge. RV deformation (strain) was measured using tissue tracking, in addition to RV ejection fraction (EF), volumes, and pulmonary regurgitant fraction. Pearson correlation coefficients were used to determine associations between both strain and CMR measures/clinical outcomes.

RESULTS: Most patients were male (11/15, 73%), with median age at TOF repair 53 days (interquartile range, 13,131). Most patients had pulmonary stenosis (vs. atresia) (11/15, 73%) and 7 (47%) received a transannular patch as part of their repair. RV function was overall preserved with mean RV EF of 62% (standard deviation [SD], 9.8). Peak radial and longitudinal strain were overall diminished (mean ± SD, 33.80 ± 18.30% and -15.50 ± 6.40%, respectively). Longer hospital length of stay after TOF repair was associated with worse RV peak radial ventricular strain (correlation coefficient (r), -0.54; p = 0.04). Greater pulmonary regurgitant fraction was associated with shorter time to peak radial RV strain (r = -0.55, p = 0.03).

CONCLUSIONS: In this small study, our findings suggest presence of early decrease in RV strain after TOF repair and its association with hospital stay when changes in EF and RV size are not yet apparent.

Keywords: Cardiac magnetic resonance imaging; Myocardial deformation; Post-operative outcomes

Author Contributions

Conceptualization: Srinivasan R, DeCost G, DiLorenzo M, Fogel M, Mercer-Rosa L; Data curation: Srinivasan R, Faerber JA, DeCost G, Fogel M, Mercer-Rosa L; Formal analysis: Faerber JA, Zhang X; Investigation: Srinivasan R, Goldmuntz E, Fogel M; Methodology: Srinivasan R, Faerber JA, DiLorenzo M, Fogel M, Mercer-Rosa L; Project administration: DeCost G, Mercer-Rosa L; Resources: DeCost G, Goldmuntz E; Supervision: Fogel M, Mercer-Rosa L; Writing - original draft: Srinivasan R, Fogel M, Mercer-Rosa L; Writing - review & editing: Srinivasan R, Faerber JA, DeCost G, Zhang X, DiLorenzo M, Goldmuntz E, Fogel M, Mercer-Rosa L.

INTRODUCTION

Tetralogy of Fallot (TOF) is a common form of cyanotic congenital heart disease, routinely repaired during infancy.¹ With surgical repair, particularly in those patients receiving a transannular patch or right ventricle (RV) to pulmonary artery conduit, the pressure loaded RV transitions to a volume loaded state, with early establishment of pulmonary regurgitation.²⁻⁵

RV strain by echocardiogram is significantly diminished early after TOF repair, with recovery of RV function to pre-operative levels 2 years after surgery.⁶ Many studies have examined RV function years after TOF repair, rather than on RV remodeling early after surgery.^{4,7} A decrease in RV strain is known to be associated with adverse events later in life.⁸ Cardiac magnetic resonance imaging (CMR) is considered the gold-standard for monitoring changes in ventricular function, volumes and valvar regurgitation in the long-term follow up after TOF repair.^{7,9,41} These factors play a significant role in the patient's long-term mortality and morbidity.⁷ Specifically, RV dysfunction years after TOF repair is associated with worse exercise performance, increased risk for malignant arrhythmias and sudden death.^{12,13}

We have previously demonstrated that CMR is feasible in infants after TOF repair without sedation or anesthesia and found elevated RV mass and significant pulmonary regurgitation at this early stage.¹⁴ However, RV strain by CMR has not been previously reported in this population immediately after TOF repair. Given the lack of knowledge on early RV remodeling, and its impact on outcomes, we sought to describe RV strain adaptation to TOF repair using CMR tissue tracking prior to hospital discharge from admission for the TOF repair. We further sought to understand the prognostic value of CMR strain by comparing RV deformation with clinical parameters.

METHODS**Study population**

Infants with TOF were recruited as part of a prospective study.³ Patients were enrolled between March 2013 and January 2016 and underwent CMR before hospital discharge. The CMR was performed without sedation or anesthesia using the “feed and swaddle” technique and therefore performed without intravenous access or gadolinium.^{14,46} This study was approved by the Institutional Review Board and informed consent was obtained for all patients.

Infants were included if younger than 1 year of age and without medical issues that would cause the patients to be unstable in the CMR scanner. CMR was planned to occur prior to hospital discharge when patients were being fed orally and without need for intravenous medications and/or access. Patients were excluded if they were receiving artificial ventilation, had a pacemaker not CMR-compatible, and if there were any clinical signs that precluded undergoing CMR without the need for anesthesia or sedation. Complete TOF repair was defined as closure of the ventricular septal defect with or without an intervention to augment pulmonary blood flow (i.e., a transannular patch or RV to pulmonary artery conduit).

Data collection

Pre- and peri-operative data including demographics, birth history, cardiac anatomy, pulmonary valve morphology and any other echocardiographic parameters, prior procedures, extra-cardiac anomalies, genetic diagnosis and hospital length of stay were collected.¹⁴

As part of the feed and swaddle technique, electrocardiogram leads were placed on the patient pulse oximetry and ear-muffs applied, and then they were fed and swaddled in a blanket in a dark room immediately preceding imaging. The infants were placed in an immobilizer (MedVac bag; CFI Medical Solutions/Contour Fabricators, Fenton, MI, USA).

The CMR protocol included static steady state free precession axial imaging to delineate anatomy, cine steady state free precession 4-chamber and short axis to measure ventricular volumes and function, and flow assessments using phase contrast CMR across the aortic root, main and branch pulmonary arteries. Exams were prioritized to show cardiac anatomy, ventricular function and pulmonary regurgitant fraction. Pulmonary regurgitant fraction $\leq 20\%$ was considered mild, 20–40% moderate, and $> 40\%$ was considered severe.¹⁷⁾

CMR image acquisition and analysis

The CMR protocol has been previously described, but briefly, focused exams were performed on a 1.5 Tesla magnet (Siemens *Aera*), including static steady state free precession axial imaging, ventricular function (cine steady state free precession 4-chamber and short axis), and flow assessments using phase contrast cardiac magnetic resonance imaging (MRI) across the aortic root, main and branch pulmonary arteries.²⁾¹⁴⁾ CMR RV ejection fraction and volumes, flow analysis and tissue tracking measurements were performed using Circle tissue tracking software (cvi42 version 5.9; Circle Cardiovascular Imaging Inc., Calgary, Canada). The software utilizes short axis images for tracing region of interest contours in systole and diastole to calculate ejection fraction and volumes. Dedicated flow maps were performed of the aortic and pulmonary outflows to quantify flow. In addition, 4-chamber and short axis images were used for tissue tracking where the user initially traces the contours of the endocardial and epicardial surfaces in end-diastole (**Figure 1**). Reference points were marked on the upper and lower left ventricular (LV) septal insertion points in short axis as well as the atrioventricular valve planes to create appropriate maps of the RV (**Figure 1**). The tissue tracking software then generated strain maps and graphs for each radial, circumferential and longitudinal strain throughout the cardiac cycle (**Figures 2 and 3**). Training on the use of the circle software was obtained from a circle representative and tracings were checked for accuracy. Manual inspection of all contours ensured integrity of the strain data.

The following strain parameters were obtained: RV peak radial and longitudinal strain, peak radial and longitudinal systolic strain rate, time to peak strain, peak displacement and velocity of peak systolic strain. Radial strain measures changes in wall thickness and is a positive value; longitudinal strain measures changes in length and is a negative value. For each parameter, individual measurements were obtained from the RV basal, mid and apical slices from short axis, as well as RV global short axis and global long axis. Interpretation of

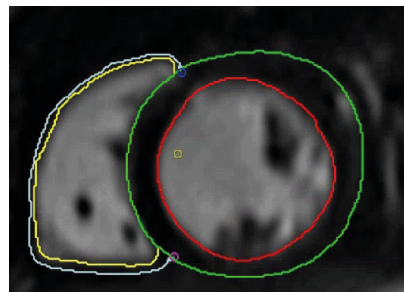


Figure 1. Endocardial and epicardial contour tracings of the right ventricle (left) and left ventricle (right) at end-diastole for calculation of strain via tissue tracking.

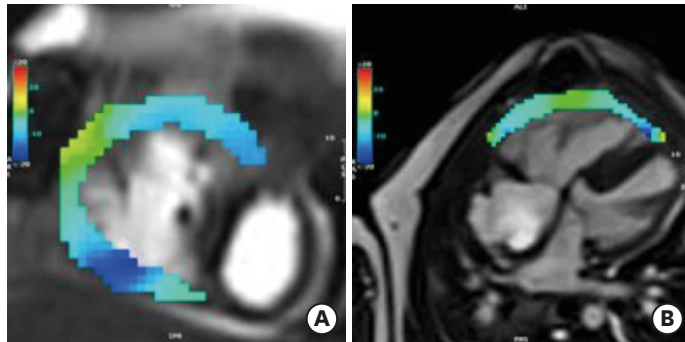


Figure 2. Representative strain maps of the right ventricle free wall in an infant with tetralogy of Fallot after repair. (A) Right ventricle short axis circumferential strain. (B) Right ventricle long axis longitudinal strain.

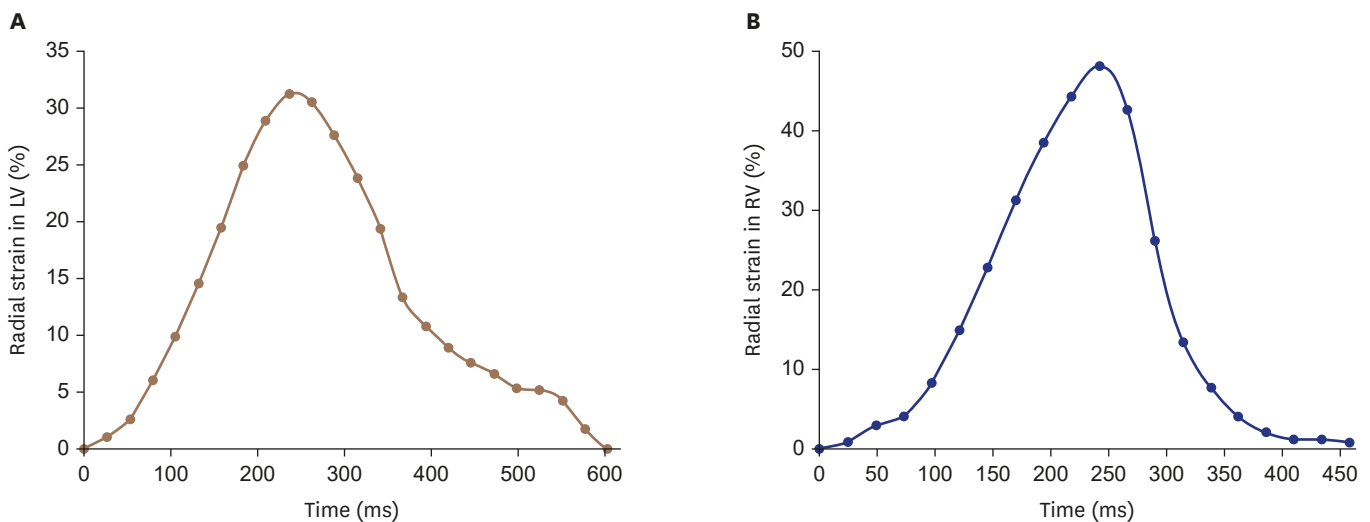


Figure 3. Graphs representing values of peak radial strain in the LV (A) and RV (B). On the left, the measurement is obtained at the maximal (peak) strain value, in this case 31%. On the right we show an example of a patient with peak radial strain of 47%. LV: left ventricle, RV: right ventricle.

normal strain values was based on previous studies of CMR RV strain, mostly from adults.¹⁸⁻²⁰⁾ Normal values for global peak longitudinal strain were defined as $-24.00 \pm 4.70\%$.¹⁸⁾¹⁹⁾²¹⁾ Peak radial strain normal was defined as $23.00 \pm 8.50\%$.²¹⁾

Statistical analysis

Patient characteristics and study variables were described using frequencies (percentages) and median (interquartile range [IQR]) or mean \pm standard deviation (SD), as appropriate. The Skewness/Kurtosis test was used to assess variable distribution. Pearson correlation coefficients were used to assess the associations between strain parameters and CMR variables, including ejection fraction, end diastolic volume indexed to body surface area (EDVi), end systolic volume indexed to body surface area and pulmonary regurgitation. Pearson correlation coefficients were also calculated for the relationship between strain parameters and hospital length of stay. Multivariable analysis was not possible due to the small sample size. Statistical significance was determined by p-values were < 0.05 . Statistical analyses were performed using SAS statistical software version 9.2 (SAS Institute, Cary, NC, USA).

RESULTS

In total, 15 patients were included in the study that had a complete research CMR. Of these, 9 were asleep for the entire exam, 2 were asleep for part of the exam, 4 were awake and one was sedated for a different procedure and remained asleep for the CMR (but did not receive additional sedation for the CMR). There were 11 males (73%) and 14 were white (93%). Most had TOF with pulmonary stenosis (11/15, 73%), while 4 patients had pulmonary atresia. One patient required BT shunt prior to TOF repair. Seven of the 15 patients received a transannular patch, 3 received a RV to pulmonary artery conduit, and 5 patients underwent pulmonary valve-sparing right ventricular outflow tract repair (non-transannular patch). One patient had 22q11.2 deletion syndrome.

The median length of stay was 7 days (IQR, 5, 12). The mean age at CMR was 93.6 days (SD ± 69) and the median time from repair to CMR was 12 days (IQR, 5, 20). Two patients had post-operative complications, including one patient who required re-operation and one patient who required cardiac catheterization. Non-cardiac complications included necrotizing enterocolitis in one patient and pneumothorax requiring intervention in 2 patients (Table 1).

On CMR, the median mycophenolic acid peak velocity was 0.9 m/sec (IQR, 0.6, 1.2), and one patient had a mild residual muscle bundle, which did not cause obstruction to flow (Table 1). There was overall mild pulmonary regurgitation with median regurgitant fraction

Table 1. Patient characteristics (n = 15)

Patient characteristics	Value
Weight (kg)	4.78 ± 1.83
Height (cm)	53.40 ± 5.25
BSA (m ²)	0.27 ± 0.06
Length of hospital stay after TOF repair (days)	7 (5, 12)
Male sex	11 (73.3)
Non-hispanic/Latino race	14 (93.3)
Pulmonary valve stenosis	11 (73.3)
Pulmonary valve atresia	4 (26.7)
Presence of LSVC to coronary sinus	1 (6.7)
Patent ductus arteriosus	8 (53.3)
Prior blalock thomas taussig shunt	1 (6.7)
Presence of extracardiac malformations	6 (43)
22q11.2 Deletion	1 (6.7)
Non-transannular patch TOF repair	5 (33.3)
Transannular patch TOF repair	7 (46.7)
Right ventricle to pulmonary artery conduit	3 (20)
Post-operative findings on cardiac magnetic resonance	
No right ventricular outflow tract obstruction	14 (93.3)
Mild pulmonary valve regurgitation*	10 (66.7)
Moderate or severe pulmonary valve regurgitation*	5 (33.3)
Peak velocity in the main pulmonary artery	0.9 (0.6, 1.2)
Cardiac magnetic resonance variables	
Right ventricular ejection fraction (%)	62.00 ± 10.00
Left ventricular ejection fraction (%)	70.00 ± 8.00
Right ventricular mass (g/m ²)	25.60 ± 9.60
Right ventricular mass Z-score	6.20 ± 2.40
RV end diastolic volume indexed (mL/m ²)	47.60 ± 13.50
RV end systolic volume indexed (mL/m ²)	25.00 ± 25.80
Pulmonary regurgitant fraction (%)	18.70 ± 18.60

All values are represented as mean ± standard deviations, median (interquartile range), or count (%).

BSA: body surface area, LSVC: left superior vena cava, TOF: Tetralogy of Fallot.

*Mild pulmonary regurgitation < 20%, moderate pulmonary regurgitation 20–40%, severe > 40%.

Table 2. Strain measurements

Measurement	Values
Global longitudinal strain (%)	-10.8 (-19.3, -6.0)
Peak radial strain (%)	35.2 (18.06, 51.12)
Peak longitudinal strain (%)	-16.51 (-19.49, -9.95)
Average time to peak radial strain (msec)	214.8 (185, 226)
Time to peak longitudinal strain (msec)	220.46 (194.4, 234)
Peak systolic radial strain rate (1/s)	2.85 (1.53, 3.63)
Peak systolic longitudinal strain rate (1/s)	-1.75 (-2.12, -1.44)
Peak systolic radial strain rate (1/s)	-2.88 (-5.7, -2.15)
Peak diastolic strain rate long (1/s)	1.61 (1.27, 2.77)
Peak displacement radial (mm)	2.01 (1.45, 3.01)
Peak displacement long (mm)	0.4 (-1.06, 1.02)
Time to peak radial (msec)	214.8 (205.5, 237)
Time to peak long (msec)	226.05 (185, 269.75)
Peak diastolic velocity radial (mm/s)	-27.65 (-38.07, -18.75)
Peak diastolic velocity long (mm/s)	-11.03 (-19.07, 28.64)

All values are presented as median (interquartile range).

Table 3. Correlation between strain variables and post-operative hospital length of stay

Strain variables	Peak radial strain	Peak longitudinal strain	Time to peak radial strain
Peak radial strain	1	-0.92 (< 0.0001)	0.48 (0.07)
Peak longitudinal strain	-0.92 (< 0.0001)	1	-0.65 (0.009)
Pulmonary regurgitant fraction	0.14 (0.62)	-0.09 (0.74)	-0.56 (0.03)
RV EDVi	0.18 (0.52)	-0.34 (0.22)	0.48 (0.07)

Values presented as Pearson correlation coefficients (p-value).

EDVi: end diastolic volume indexed to body surface area, RV: right ventricle.

of 17% (IQR, 2.4, 22.3). There were 6 patients (40%) with regurgitant fraction greater than 20%. There was no overall RV dilation with mean RV EDVi (47.60 ± 13.50 cc/m²) and overall preserved RV ejection fraction ($62.00 \pm 10.00\%$.) RV mass was significantly elevated (25.60 ± 9.60 g/m²; Z-score, 6.20 ± 2.40).

The mean RV peak longitudinal strain was lower than average norms (median [IQR], -16.51 [-19.49, -9.95]) and the RV peak radial strain had a normal median value (35.2 [18.06, 51.12]) (Table 2). Longer post-operative hospital length of stay was associated with worse RV peak radial strain ($p = 0.038$). The association of post-operative hospital length of stay with peak longitudinal strain did not reach statistical significance ($p = 0.057$). As expected, there was a strong association between RV peak longitudinal strain and RV peak radial strain (Table 3).

There was a moderate association between pulmonary regurgitation and shorter time to peak radial strain ($r = -0.56$, $p = 0.03$), but not with peak radial or longitudinal strain. The association between RV EDVi with longer RV time to peak radial strain did not reach statistical significance ($r = 0.48$, $p = 0.07$) (Table 3).

DISCUSSION

In this study, we examined RV deformation and its relationship with post-operative outcomes in infants early after TOF repair utilizing un-sedated CMR. Our main CMR findings included: 1) Significantly increased RV mass, overall preserved RV ejection fraction and mild pulmonary regurgitation; 2) Lower than normal median longitudinal RV strain; 3) Association between peak radial strain with longer hospital length of stay; and 4) Association between pulmonary regurgitation and shorter time to peak radial strain.

This study is unique in performing strain in CMRs early after TOF repair, and to our knowledge, there are no similar studies to compare this finding. Specifically, this study is novel in describing radial strain in this patient population. Radial strain reflects thickening of the RV wall, and longitudinal strain reflects base to apex deformation. Cardiac MRI plays a unique role in 3-dimensional imaging and the ability to calculate RV radial strain, which is not feasible with transthoracic echocardiography.

Previous studies have reported that reduced strain is associated with worse outcomes in disease processes that impact the RV, but very few studies have tracked these changes early in the post-operative course.⁸⁾²²⁾ Previous reports in TOF suggest that RV strain deteriorates prior to changes in ejection fraction, and this might be the case in the present study.²³⁾ These patients also had significantly elevated RV mass, which may play a role in altered loading conditions and thus worsened strain. In older patients with repaired TOF, worse LV and RV strain are associated with adverse outcomes, including sudden cardiac death and aborted-cardiac death.⁸⁾ Thus, strain seems to be a more sensitive parameter of RV function than ejection fraction.

We also found that abnormal RV strain was associated with increased length of stay following repair. This finding has been reported in other forms of congenital heart disease, such as transposition of the great arteries, where abnormal LV strain correlated with increased length of stay after repair.²⁴⁾ In adults with heart failure, worse RV strain is associated with increased risk of readmissions and death.²⁵⁾²⁶⁾ Although prior studies have described the association of RV echocardiography strain early after TOF repair with length of stay, to our knowledge, this is the first study that suggests an association between MRI strain with length of stay after TOF repair. Further, the association between RV radial strain and length of stay is novel. This underlies the clinical implications of subtle changes in RV function as detected by tissue tracking and its association with clinical outcomes. Although the long-term consequences of early RV dysfunction after TOF repair are yet to be studied, efforts should be made towards optimizing RV function in the peri-operative period.

In addition, there was a negative correlation between pulmonary regurgitation and shorter time to peak radial strain. Although this group of patients had overall normal RV end-diastolic volumes, changes in time to peak strain may reflect changes in loading conditions before they incur changes in RV volume. Corroborating our findings, studies have shown that with increased RV loading conditions (as is the case with pulmonary regurgitation), there is slower radial motion of the RV. This reflects in abnormal RV wall thickening as evidenced by radial strain, and to a lesser degree, the base to apex movement of RV contraction as evidenced by longitudinal strain.²²⁾²⁷⁾

In a prior report from our group investigating changes in RV strain by echocardiography, we demonstrated that RV strain was significantly diminished early after TOF repair with recovery to pre-operative values 2 years after TOF surgery.⁶⁾ Likewise, the present study suggests subtle changes in RV deformation early after TOF repair and highlights the association between RV strain and length of hospital stay. The long-term consequences of RV dysfunction early after TOF repair are yet to be studied, and efforts should be made towards optimizing RV function in the peri-operative period.

Limitations: this study was limited by a small sample size; thus, we limited the analyses to correlations. The reference values used in this study are derived from adult controls. This was unavoidable because it is unusual for normal infants to undergo CMR at this age so that

normal data can be obtained. From a technical standpoint, the sequences were free-breathing, and thus image quality might have been lower than that which is obtained with the patient under sedation, although we were able to make strain calculations in all 15 patients. Despite these limitations, we believe that our findings are informative to this patient population.

In conclusion, this small study we present the early RV deformation status in patients undergoing TOF repair using un-sedated CMR. Our findings suggest presence of early decrease in RV strain after TOF repair when changes in ejection fraction and RV size are not apparent. The association with longer hospital length of stay and the long-term consequences of these early findings require validation in larger studies with longitudinal follow up.

REFERENCES

1. Bailliard F, Anderson RH. Tetralogy of Fallot. *Orphanet J Rare Dis* 2009;4:2.
[PUBMED](#) | [CROSSREF](#)
2. Mercer-Rosa L, Pinto N, Yang W, Tanel R, Goldmuntz E. 22q11.2 Deletion syndrome is associated with perioperative outcome in tetralogy of Fallot. *J Thorac Cardiovasc Surg* 2013;146:868-73.
[PUBMED](#) | [CROSSREF](#)
3. Mercer-Rosa L, Elci OU, DeCost G, et al. Predictors of length of hospital stay after complete repair for tetralogy of Fallot: a prospective cohort study. *J Am Heart Assoc* 2018;7:e1-13.
[PUBMED](#) | [CROSSREF](#)
4. Annavajjhala V, Punn R, Tacy TA, Hanley FL, McElhinney DB. Serial assessment of postoperative ventricular mechanics in young children with tetralogy of Fallot: comparison of transannular patch and valve-sparing repair. *Congenit Heart Dis* 2019;14:691-9.
[PUBMED](#) | [CROSSREF](#)
5. Quansheng X, Qin WU, Wei L, Yueyi R, Qian C. Primary surgical repair of tetralogy of Fallot in symptomatic neonates and premature infants. *Chinese J Thorac Cardiovasc Surg* 2017;33:262-6.
6. DiLorenzo MP, Elci OU, Wang Y, et al. Longitudinal changes in right ventricular function in tetralogy of Fallot in the initial years after surgical repair. *J Am Soc Echocardiogr* 2018;31:816-21.
[PUBMED](#) | [CROSSREF](#)
7. Knauth AL, Gauvreau K, Powell AJ, et al. Ventricular size and function assessed by cardiac MRI predict major adverse clinical outcomes late after tetralogy of Fallot repair. *Heart* 2008;94:211-6.
[PUBMED](#) | [CROSSREF](#)
8. Orwat S, Diller GP, Kempny A, et al. Myocardial deformation parameters predict outcome in patients with repaired tetralogy of Fallot. *Heart* 2016;102:209-15.
[PUBMED](#) | [CROSSREF](#)
9. Kilner PJ, Geva T, Kaemmerer H, Trindade PT, Schwitter J, Webb GD. Recommendations for cardiovascular magnetic resonance in adults with congenital heart disease from the respective working groups of the European Society of Cardiology. *Eur Heart J* 2010;31:794-805.
[PUBMED](#) | [CROSSREF](#)
10. Antonov NK, Ruzal-Shapiro CB, Morel KD, et al. Feed and wrap MRI technique in infants. *Clin Pediatr (Phila)* 2017;56:1095-103.
[PUBMED](#) | [CROSSREF](#)
11. Valente AM, Geva T. How to image repaired tetralogy of Fallot. *Circ Cardiovasc Imaging* 2017;10:e004270.
[PUBMED](#) | [CROSSREF](#)
12. Dennis M, Moore B, Kotchetkova I, Pressley L, Cordina R, Celermajer DS. Adults with repaired tetralogy: low mortality but high morbidity up to middle age. *Open Heart* 2017;4:e000564.
[PUBMED](#) | [CROSSREF](#)
13. Geva T, Sandweiss BM, Gauvreau K, Lock JE, Powell AJ. Factors associated with impaired clinical status in long-term survivors of tetralogy of Fallot repair evaluated by magnetic resonance imaging. *J Am Coll Cardiol* 2004;43:1068-74.
[PUBMED](#) | [CROSSREF](#)
14. DiLorenzo MP, Goldmuntz E, Nicolson SC, Fogel MA, Mercer-Rosa L. Early postoperative remodelling following repair of tetralogy of Fallot utilising unsedated cardiac magnetic resonance: a pilot study. *Cardiol Young* 2018;28:697-701.
[PUBMED](#) | [CROSSREF](#)

15. Fogel MA, Pawlowski TW, Harris MA, et al. Comparison and usefulness of cardiac magnetic resonance versus computed tomography in infants six months of age or younger with aortic arch anomalies without deep sedation or anesthesia. *Am J Cardiol* 2011;108:120-5.
[PUBMED](#) | [CROSSREF](#)
16. Shariat M, Mertens L, Seed M, et al. Utility of feed-and-sleep cardiovascular magnetic resonance in young infants with complex cardiovascular disease. *Pediatr Cardiol* 2015;36:809-12.
[PUBMED](#) | [CROSSREF](#)
17. Orwat S, Diller GP, Kempny A, et al. Myocardial deformation parameters predict outcome in patients with repaired tetralogy of Fallot. *Heart* 2016;102:209-15.
[PUBMED](#) | [CROSSREF](#)
18. Taylor RJ, Moody WE, Umar F, et al. Myocardial strain measurement with feature-tracking cardiovascular magnetic resonance: normal values. *Eur Heart J Cardiovasc Imaging* 2015;16:871-81.
[PUBMED](#) | [CROSSREF](#)
19. Peng J, Zhao X, Zhao L, et al. Normal values of myocardial deformation assessed by cardiovascular magnetic resonance feature tracking in a healthy Chinese population: a multicenter study. *Front Physiol* 2018;9:1181.
[PUBMED](#) | [CROSSREF](#)
20. Mercer-Rosa L, Yang W, Kutty S, Rychik J, Fogel M, Goldmuntz E. Quantifying pulmonary regurgitation and right ventricular function in surgically repaired tetralogy of Fallot: a comparative analysis of echocardiography and magnetic resonance imaging. *Circ Cardiovasc Imaging* 2012;5:637-43.
[PUBMED](#) | [CROSSREF](#)
21. Liu T, Wang C, Li S, Zhao Y, Li P. Age- and gender-related normal references of right ventricular strain values by tissue tracking cardiac magnetic resonance: results from a Chinese population. *Quant Imaging Med Surg* 2019;9:1441-50.
[PUBMED](#) | [CROSSREF](#)
22. Haeck ML, Scherptong RW, Marsan NA, et al. Prognostic value of right ventricular longitudinal peak systolic strain in patients with pulmonary hypertension. *Circ Cardiovasc Imaging* 2012;5:628-36.
[PUBMED](#) | [CROSSREF](#)
23. Scherptong RWC, Mollema SA, Blom NA, et al. Right ventricular peak systolic longitudinal strain is a sensitive marker for right ventricular deterioration in adult patients with tetralogy of Fallot. *Int J Cardiovasc Imaging* 2009;25:669-76.
[PUBMED](#) | [CROSSREF](#)
24. Meier GD, Bove AA, Santamore WP, Lynch PR. Contractile function in canine right ventricle. *Am J Physiol* 1980;239:H794-804.
[PUBMED](#) | [CROSSREF](#)
25. Pletzer SA, Atz AM, Chowdhury SM. The relationship between pre-operative left ventricular longitudinal strain and post-operative length of stay in patients undergoing arterial switch operation is age dependent. *Pediatr Cardiol* 2019;40:366-73.
[PUBMED](#) | [CROSSREF](#)
26. Hamada-Harimura Y, Seo Y, Ishizu T, et al. Incremental prognostic value of right ventricular strain in patients with acute decompensated heart failure. *Circ Cardiovasc Imaging* 2018;11:e007249.
[PUBMED](#) | [CROSSREF](#)
27. Smith BC, Dobson G, Dawson D, Charalampopoulos A, Grapsa J, Nihoyannopoulos P. Three-dimensional speckle tracking of the right ventricle: toward optimal quantification of right ventricular dysfunction in pulmonary hypertension. *J Am Coll Cardiol* 2014;64:41-51.
[PUBMED](#) | [CROSSREF](#)